Fluid Dynamics & Materials Processing
DOI:10.32604/fdmp.2020.09010
Article

Oscillations of an Inviscid Encapsulated Drop

Aleksandr Shiryaev*

Ishlinsky Institute for Problems in Mechanics of the Russian Academy of Sciences, Moscow, 119526, Russia
*Corresponding Author: Aleksandr Shiryaev. Email: aashiryaev@list.ru
Received: 01 November 2019; Accepted: 05 February 2020

Abstract: The problem relating to the small-amplitude free capillary oscillations of an encapsulated spherical drop is solved theoretically in the framework of asymptotic methods. Liquids are supposed to be inviscid and immiscible. The formulas derived are presented for different parameters of the inner and outer liquids, including densities, thickness of the outer liquid layer, and the surface and interfacial tension coefficients. The frequencies of oscillation of the encapsulated drop are studied in relation to several "modes" which can effectively be determined in experiments by photo and video analysis. The results are presented in terms of oscillation frequencies reported as a function of the mode number, the spherical layer thickness and the relation between the (surface and interfacial) tension coefficients. It is revealed that the influence of the liquids' parameters (and related variations) on the drop oscillation changes dramatically depending on whether oscillations are "in-phase" or "out-of-phase". Frequencies for "in-phase" type oscillations can be correlated with linear functions of the shell thickness and the relative values of interfacial tension coefficient whereas the analogous dependencies for the "out-of-phase" type oscillation are essentially non-linear.

Keywords: Encapsulated drop; oscillation frequencies; inviscid fluid

1 Introduction

Encapsulated drop is a compound drop, consisting of an inner liquid, surrounded by another immiscible liquid layer. Such drops are common phenomenon in metallurgy, chemical engineering and are observed in biological structures. Encapsulated drops have been studied extensively for almost half of a century. One of the first investigations of oscillations are thin film stability considerations [1]. Oscillations of a stratified compound drop were studied theoretically [2] and previous experimental facts were summarized [3]. Later, oscillations of a compound drop were studied theoretically for some more complex cases, including effects of drop's rotation [4], free surface oscillation amplitude dampening [5] and oscillation stability [6].

Further investigations consider additional effects, which were studied extensively by numerical analysis. Dynamics of encapsulated drop and its usefulness in medical applications were presented [7]. Here, a set of papers, considering external shear flows should be mentioned, including [8,9], in which compound drop's deformation and effect of inner liquid eccentricity were studied. Such drop's dynamic properties allow using them as transport for liquids, so different aspects of encapsulated drop's motion are actively studied

This work is licensed under a Creative Commons Attribution 4.0 International License, which permits unrestricted use, distribution, and reproduction in any medium, provided the original work is properly cited.

[10–12]. New numerical method, considering particle hydrodynamics in encapsulated drop was developed [13]. Nonlinear oscillations were studied by numerical methods, as well [14].

Nowadays, methods for producing encapsulated drops with thin shells of outer liquid using microfluidic devices in different designs were developed [15–18], and are studied numerically to enhance their effectiveness [19] There's a clear demand of thorough theoretical analysis on encapsulated drops' problem. Analysis of internal flows in liquid drop is a complicated task, which is usually studied by numerical methods even in a non-compound drop case [20,21]. However, investigation of oscillation spectrum can be useful in determination of inner properties of a compound drop [22,23], as well as oscillation effects on stability and motion of encapsulated drops. Most papers consider second mode of oscillations or give only thin layer approximation [2,24]. High resolution images of oscillating drops show that simultaneous multiple mode drop oscillations are common thing in laboratory experiments [25,26], as well as in field observations [27]. The goal of the current study is to analyze encapsulated drop oscillation frequencies of several lower modes, which can be observed in experiments, and determine their dependencies on inner and outer liquid's parameters. In addition, simplified expressions for frequencies will be investigated for errors and applicability in quantitative considerations.

2 Statement of the Problem

Encapsulated drop with radius R is considered as a two-layer liquid system, which in equilibrium state has the form of a spherical drop of inner liquid, covered by concentric spherical layer of dissimilar outer liquid. Spherical layer is thin and has a finite thickness h. This system (Fig. 1) accomplishes small-amplitude free capillary oscillations. The both liquids are assumed to be inviscid and incompressible. Outer liquid density is ρ_o and inner one is ρ_i. The free surface tension coefficient is σ_o and σ_i is the interfacial tension coefficient. Further, the index "o" refers to the outer liquid or to the free surface of the outer liquid and index "i" to the liquid in the inner drop or the internal liquid–liquid interface.

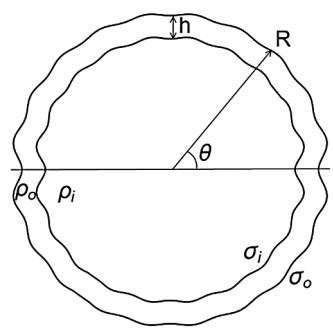

Figure 1: Oscillating encapsulated drop illustration

3 Governing Equations

The problem is formulated in spherical coordinates $\{r, \theta, \varphi\}$ with an origin at the drop mass center. The Consideration is restricted to axisymmetric oscillations, so all variables' dependencies on orbital angle φ can be ignored. Free surface and interfacial surface are defined by the following equations respectively: $F_o(r, \theta, t) \equiv r - R - \xi_o(\theta, t) = 0$ and $F_i(r, \theta, t) \equiv r - R + h - \xi_i(\theta, t) = 0$. Here, $\xi_o(\theta, t)$ and $\xi_i(\theta, t)$ are time-dependent functions which describe shapes of the oscillating surfaces.

Euler's equations for inner and outer liquids and continuity equations are as follows

$$\rho_{i,o}\left(\frac{\partial \vec{V}_{i,o}}{\partial t} + \vec{V}_{i,o}(\nabla \vec{V}_{i,o})\right) = -\nabla P_{i,o} \tag{1}$$

$$\operatorname{div} \vec{V}_{i,o} = 0 \tag{2}$$

where $\vec{V}_{i,o}$ are flow velocities, $P_{i,o}$ are hydrodynamic pressures. The equations are supplemented with condition of flow velocity finiteness at the drop mass center

$$r \to 0: \qquad \left|\vec{V}_2\right| < \infty \tag{3}$$

Kinematic and dynamic boundary conditions on a free surface are given by

$$r = R + \xi_o(\theta, t): \qquad \frac{dF_o(r,\theta,t)}{dt} = 0; \tag{4}$$

$$r = R + \xi_o(\theta, t): \qquad P_o - P_{\sigma o} = P_{ext}. \tag{5}$$

Here, P_o is a hydrodynamic pressure in outer liquid layer, $P_{\sigma o} = \sigma_o \operatorname{div} \vec{n}_o$ is a capillary pressure on a free surface, P_{ext} is an external hydrostatic pressure outside the drop and $\vec{n}_o \equiv \nabla F_o(r,\theta,t)/|\nabla F_o(r,\theta,t)|_{F_o=0}$ is a free surface normal.

Boundary conditions at the liquid-liquid interface are kinematic and dynamic ones, and the condition of continuity of the normal velocity component which have the following form

$$r = R - h + \xi_i(\theta, t): \qquad \frac{dF_i(r,\theta,t)}{dt} = 0; \tag{6}$$

$$r = R - h + \xi_i(\theta, t): \qquad P_i - P_{\sigma i} = P_o; \tag{7}$$

$$r = R - h + \xi_i(\theta, t): \qquad \vec{V}_o \cdot \vec{n}_i = \vec{V}_i \cdot \vec{n}_i. \tag{8}$$

Here, P_i is a hydrodynamic pressure in inner liquid, $P_{\sigma i} = \sigma_i \operatorname{div} \vec{n}_i$ and $\vec{n}_i \equiv \nabla F_i(r,\theta,t)/|\nabla F_i(r,\theta,t)|_{F_i=0}$ is a capillary pressure on a interfacial surface and its normal, respectively.

The problem is supplemented with the conditions of conservation of the inner liquid and overall drop volume, as well as immobility of the drop mass center under oscillations of the drop surface which can be written as

$$\int_0^{2\pi}\int_0^{\pi}\int_0^{R-h+\xi_i(\theta,t)} r^2 \sin\theta \mathrm{d}r\mathrm{d}\theta\mathrm{d}\varphi = \frac{4}{3}\pi\rho(1-h)^3$$

$$\int_0^{2\pi}\int_0^{\pi}\int_0^{R+\xi_o(\theta,t)} r^2 \sin\theta \mathrm{d}r\mathrm{d}\theta\mathrm{d}\varphi = \frac{4}{3}\pi \tag{9}$$

$$\int_0^{2\pi}\int_0^{\pi}\int_0^{R-h+\xi_i(\theta,t)} \rho_i \vec{r} r^2 \sin\theta \mathrm{d}r\mathrm{d}\theta\mathrm{d}\varphi + \int_0^{2\pi}\int_0^{\pi}\int_{1-h+\xi_i(\theta,t)}^{1+\xi_o(\theta,t)} \rho_o \vec{r} r^2 \sin\theta \mathrm{d}r\mathrm{d}\theta\mathrm{d}\varphi = \vec{0}$$

4 Scalarization and Linearization

The problem will be solved under the assumption that equilibrium surface distortion $\xi_{i,o}(\theta, t)$ we are interested in is small, the model of a potential liquid flow is used, in terms of which velocity fields $\vec{V}_{i,o}$ are determined by hydrodynamic potential $\psi_{i,o}(r,\theta,t)$: $\vec{V}_{i,o} = \nabla\psi_{i,o}(r,\theta,t)$. Since small oscillations of the

surfaces are considered we can assume that, $\max\left|\xi_{i,o}(\theta,t)\right|/R \equiv \varepsilon << 1$, and, as a consequence, the velocity of a liquid flow induced by surface oscillations is also small. Therefore, we can assume $\left|\psi_{i,o}(r,\theta,t)\right| \sim \left|\xi_{i,o}(\theta,t)\right|$. The consideration will be restricted by the ε^0 and ε^1 orders of smallness in amplitude, and the desired quantities will be represented as sums of components of the above orders of magnitude. For the sake of convenience of calculations, we will go over to dimensionless variables assuming that $R = 1$, $\rho_o = 1$, and $\sigma_o = 1$. The designations of the dimensionless variables will remain the same. After the standard procedures of scalarization and linearization on the set of Eqs. (1)–(9) zeroth- and first-order problems can be obtained.

5 Equilibrium Drop. Zeroth-Order Problem

Zeroth-order problem consists of scalarized Euler's equations and dynamic boundary conditions. Solution of this system gives hydrostatic pressures in outer $P_o{}^{(0)} = P_{ext} + 2$ and inner $P_i{}^{(0)} = \dfrac{2}{1-h}\sigma + P_{ext} + 2$ liquids of an undisturbed encapsulated drop. Here and after top Arabic number in round brackets indicates order of amplitude smallness ε.

6 Oscillating Drop. First-Order Problem

Scalarized and linearized first-order equation system in nondimensional variables is given by the following set of equations and boundary conditions.

Hydrodynamic pressures obtained from Eq. (1) are given as

$$P_o^{(1)} = -\frac{\partial \psi_o}{\partial t}; \tag{10}$$

$$P_i^{(1)} = -\rho\,\frac{\partial \psi_i}{\partial t};$$

Here, $\rho \equiv \rho_i/\rho_0$ is a nondimensional parameter, characterizing relative density of inner liquid. Laplace equations and condition of velocity limitness obtained from (2) and (3) can be written as

$$\Delta\psi_o = 0$$

$$\Delta\psi_i = 0 \tag{11}$$

$$r \to 0: \qquad |\nabla\psi_i| < \infty;$$

Kinematic (4), (6) and continuity of the normal velocity component (8) boundary conditions are given as

$$r = 1: \quad -\frac{\partial \xi_o(\theta,t)}{\partial t} + \frac{\partial \psi_o}{\partial r} = 0;$$

$$r = 1-h: \quad -\frac{\partial \xi_i(\theta,t)}{\partial t} + \frac{\partial \psi_i}{\partial r} = 0 \tag{12}$$

$$r = 1-h: \quad \frac{\partial \psi_o}{\partial r} = \frac{\partial \psi_i}{\partial r}.$$

Dynamic boundary conditions (5), (7) are obtained by

$$r = 1-h: \quad P_i{}^{(1)} - P_{\sigma i}{}^{(1)} = P_o{}^{(1)} \tag{13}$$

$$r = 1: \quad P_o{}^{(1)} - P_{\sigma o}{}^{(1)} = 0$$

Corrections to capillary pressures have the following form

$$P_{\sigma o}^{(1)} = -2\xi_o(\theta, t) - \Delta_\theta \xi_o(\theta, t); \tag{14}$$

$$P_{\sigma i}^{(1)} = \sigma \frac{-2\xi_i(\theta, t) - \Delta_\theta \xi_i(\theta, t)}{(1-h)^2};$$

where $\Delta_\theta \equiv \frac{1}{\sin\theta}\frac{\partial}{\partial\theta}\left(\sin\theta\,\frac{\partial}{\partial\theta}\right)$ and $\sigma \equiv \sigma_i/\sigma_0$. The equations are supplemented by additional integral conditions (9) which can be written as

$$\frac{2\pi}{3}\int_0^\pi (3\xi_i(\theta, t))(1-h)^2 \sin\theta \mathrm{d}\theta = 0$$

$$\frac{2\pi}{3}\int_0^\pi 3\xi_o(\theta, t)\sin\theta\,\mathrm{d}\theta = 0 \tag{15}$$

$$\int_0^{2\pi}\int_0^\pi \rho\frac{1}{4}(1-h+4\xi_i(\theta, t))\cos\theta\sin\theta \mathrm{d}\theta\mathrm{d}\varphi +$$

$$+\int_0^{2\pi}\int_0^\pi \frac{1}{4}(h+4\xi_o(\theta, t)-4\xi_i(\theta, t))\cos\theta\sin\theta \mathrm{d}\theta\mathrm{d}\varphi = 0$$

Shape functions of a free surface $\xi_o(\theta, t)$ and liquid-liquid interface $\xi_i(\theta, t)$ are sought in the form of an expansion in Legendre polynomials $P_n(\mu)$ where $\mu \equiv \cos\theta$ and are given as

$$\xi_o(\theta, t) = \sum_{n=0}^{\infty} \alpha_n(t) P_n(\mu) \tag{16}$$

$$\xi_i(\theta, t) = \sum_{n=0}^{\infty} \beta_n(t) P_n(\mu)$$

Solutions of Laplace's equations with boundary condition (11) gives hydrodynamic potentials $\psi_{i,o}(r, \theta, t)$ which have the following form

$$\psi_o(r, \theta, t) = \sum_{n=0}^{\infty} A_n(t) r^n P_n(\theta) + \sum_{n=0}^{\infty} B_n(t) r^{-(n+1)} P_n(\mu); \tag{17}$$

$$\psi_i(r, \theta, t) = \sum_{n=0}^{\infty} V_n(t) r^n P_n(\mu);$$

Expressions (16)–(17) are substituted into conditions (12) which are solved taking into account the orthogonality of Legendre polynomials. Solutions of this system determine coefficients A_n, B_n, V_n as functions of $\alpha_n(t)$ and $\beta_n(t)$ are obtained by

$$B_n = \frac{(1-h)(\alpha_n{}'(t) - \beta_n{}'(t))}{(-(1-h)^{-2n} + 1 - h)(1+n)}$$

$$A_n = \frac{\alpha_n{}'(t) - \dfrac{(1-h)(\alpha_n{}'(t) - \beta_n{}'(t))}{-1 + (1-h)^{-2n} + h}}{n} \tag{18}$$

$$V_n = \frac{\beta_n{}'(t)}{n}$$

Integral conditions (15) determine coefficients for expressions (16): $\alpha_0(t) = 0$, $\beta_0(t) = 0$, $\rho_1\alpha_1(t) + (\rho_2 - \rho_1)\beta_1(t) = 0$.

Hydrodynamic (10) and capillary (14) pressures are determined considering expressions (16)–(18) and can be written as

$$P_o^{(1)} = -\left(\sum_{n=0}^{\infty} r^n P_n(\mu) A_n{}'(t) + \sum_{n=0}^{\infty} r^{-1-n} P_n(\mu) B_n{}'(t)\right)$$

$$P_i^{(1)} = -\rho \sum_{n=0}^{\infty} r^n P_n(\mu) V_n{}'(t) \tag{19}$$

$$P_{\sigma o}^{(1)} = \sum_{n=2}^{\infty} (n-1)(n+2)\alpha_n(t) P_n(\mu)$$

$$P_{\sigma o}^{(1)} = \left(\frac{\sigma}{(-1+h)^2}\right) \sum_{n=2}^{\infty} (n-1)(n+2)\beta_n(t) P_n(\mu)$$

Expressions (19) are substituted into dynamic boundary conditions (13), which can be represented respectively as follows

$$C_1(n)\alpha_n(t) + C_2(n)\alpha_n{}''(t) + C_3(n)\,\beta_n{}''(t) = 0 \tag{20}$$

$$C_4(n)\beta_n(t) + C_5(n)\alpha_n{}''(t) + C_6(n)\,\beta_n{}''(t) = 0$$

Here, $C_k(n)$ are quite cumbersome numerical coefficients, which depend on ρ, h, σ and are represented in Appendix A. System (20) is simplified to obtain equation for the $\alpha_n(t)$, which describes evolution of oscillations of the free surface which is given as

$$D_1(n)\alpha_n(t) + D_2(n)\alpha_n{}''(t) + D_3(n)\alpha_n{}^{(4)}(t) = 0 \tag{21}$$

Here, coefficients $D_k(n)$ have the following expressions: $D_1(n) = -\dfrac{C_1(n)}{C_3(n)}$, $D_2(n) = -\dfrac{C_2(n)}{C_3(n)} - \dfrac{C_1(n)C_6(n)}{C_3(n)C_4(n)}$ and $D_3(n) = \dfrac{C_5(n)}{C_4(n)} - \dfrac{C_2(n)C_6(n)}{C_3(n)C_4(n)}$. Second equation of the system gives $\beta_n(t)$ as a function of $\alpha_n(t)$ and will not be considered further, because it determines oscillations of "inner" liquid-liquid interface.

7 Frequency Analysis

Equation, which determines free surface oscillation frequencies $\omega_n(t)$, can be found from the fourth-order differential Eq. (21) by substituting $\alpha_n(t) = E_n \cos(\omega_n t + \phi_n)$. Solutions of the resulting biquadratic equation are given as

$$\omega_n = \frac{1}{\sqrt{2}} \sqrt{\frac{D_2(n)}{D_3(n)} \pm \frac{\sqrt{D_2(n)^2 - 4D_3(n)D_1(n)}}{D_3(n)}} \tag{22}$$

Numerical calculations will be represented for the case of water drop, encapsulated in a thin layer of silicone oil with normal temperature and pressure. Surface tension coefficients for water and silicone oil are $73 \cdot 10^{-3}$ N/m and $20 \cdot 10^{-3}$ N/m respectively, so dimensionless parameter $\sigma = \frac{73-20}{20} = 2.65$. Relative density parameter $\rho = \frac{\rho_i}{\rho_o} = \frac{1}{0.95} = 1.05$. Since the present paper studies encapsulated drops with a thin layer of outer liquid, thicknesses $h < 0.1\ R$ will be considered.

Fig. 2 shows two frequencies corresponding to two oscillation modes: "in-phase" mode, when drop's free and internal surfaces oscillate generally like homogeneous liquid, and "out-of-phase" mode, which is typical for two-layered liquids.

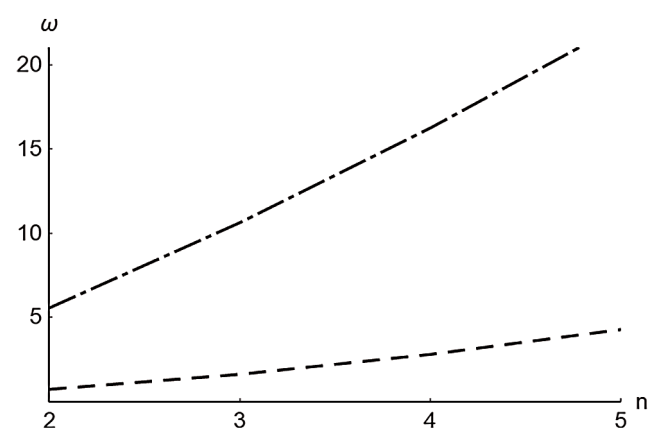

Figure 2: Free capillary oscillation frequencies of an encapsulated drop as a function of mode number n. Dashed line – "out-of-phase" mode, dash-dotted – "in-phase" mode

Further analysis will consider $\delta \equiv \frac{\omega}{\sqrt{n(n-1)(n+2)}}$ which is normalized oscillation frequency. Such normalization allows displaying frequencies of several modes in a single figure, as well as showing frequency values, relative to that of a homogeneous drop consisting of outer shell liquid, $\omega_R = \sqrt{n(n-1)(n+2)}$, which can be easily derived from [28]. Fig. 3 shows that encapsulated drop oscillation "in-phase" frequencies are greater than those for homogeneous drop. Increase in outer liquid layer thickness h has greater effect on higher modes of oscillations, decreasing values of δ. These dependencies can be reasonably approximated by linear functions, derived from the exact solutions (22) are obtained by

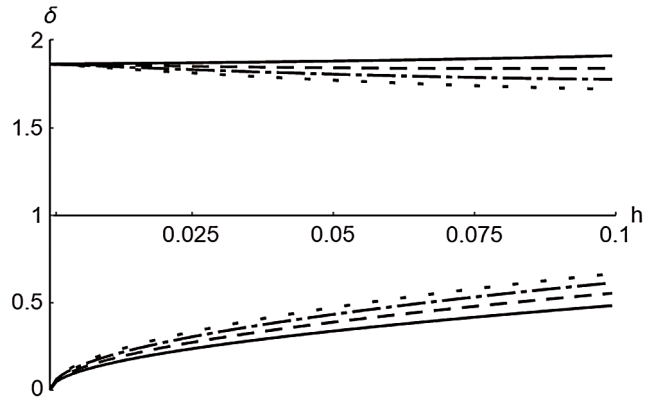

Figure 3: Normalized oscillation frequencies of an encapsulated drop as functions of spherical layer thickness h. 4 curves at the top-"In-phase" mode. 4 curves at the bottom-"Out-of-phase" mode. Solid line – oscillation mode number n = 2, dashed line – n = 3, dash-dotted – n = 4 and dotted – n = 5

$$\omega \approx \omega_R \left(\sqrt{\rho(1+\sigma)} + h \frac{\rho(-1+\rho+2\sigma+3\sigma^2) + n\left(\rho^2 - (1+\sigma)^2\right)}{2(\rho(1+\sigma))^{3/2}} \right) \tag{23}$$

Such approximation works well for lower modes of oscillations, but error is increasing with mode number and shell thickness, reaching values up to several percent.

For the case of "out-of-phase" oscillations frequencies are significantly lower than ω_R, and thinner encapsulation shell will result in further decrease in ω_n (Fig. 3). In this case, asymptotic decomposition for oscillation frequency contains only semi-integer orders of h, and simplest approximate expression $\omega \approx \omega_R \sqrt{h} \sqrt{\frac{\sigma(1+n)}{1+\sigma}}$ agrees well with the exact solution (22). Difference in evaluated exact and approximate values is less than 3%.

Inner and outer liquids may have closer values of surface tension coefficients (for example, inner liquid is aniline with coefficient of surface tension equal to $42 \cdot 10^{-3}$ N/m and therefore $\sigma \approx 1$). In that case, frequencies in "in-phase" mode are getting closer to ω_R with lower values of σ as shown in Fig. 4. These dependencies can be roughly approximated within $0.5 < \sigma < 3$ with the following linear expression $\omega \approx \omega_R \left(\sqrt{\rho} + \frac{h}{2\rho^{3/2}} \left(n\left(\rho^2 - 1\right) - \rho + \rho^2 \right) + \left(\frac{\sqrt{\rho}}{2} + \frac{h}{4\rho^{3/2}} \left(+7\rho - 3\rho^2 - n\left(1 + 3\rho^2\right) \right) \right) \sigma \right)$. Dependencies $\delta(\sigma)$ represented in Fig. 4 show that decrease of σ lower "out-of-phase" oscillation frequency, making it even more differ from ω_R. Lower lines in Fig. 4 have nonlinear dependency, which can be approximately expressed by $\omega \approx \omega_R \sqrt{h\,(1+n)\,\sigma}$.

Inner and outer liquid's densities are the thing to consider, when "in-phase" mode is investigated. Numerical analysis shows that greater values of ρ correspond to lower oscillation frequencies. This dependency tends to be nonlinear, according to both exact (22) and approximate (23) expressions. However, when liquid's densities differ not more than 20% frequency can be approximated by a linear function of ρ because numerically obtained curves are almost linear. "Out-of-phase" mode oscillations slightly decrease with greater ρ. However, values of $\frac{\partial \delta}{\partial \rho}$ are about 1–2% for 1 < ρ < 1.2. It means that values of δ are almost constant, and this dependency may be neglected in practical applications.

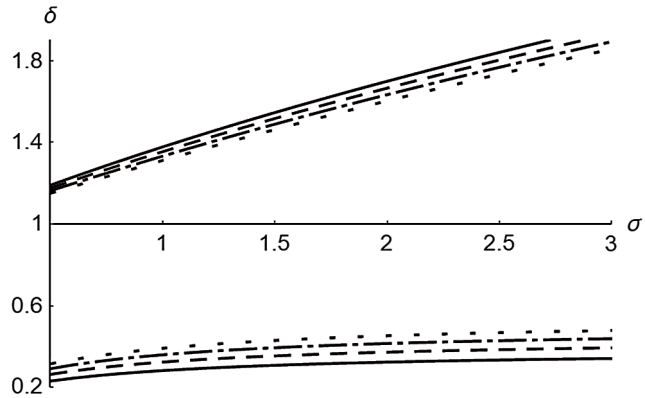

Figure 4: Normalized oscillation frequencies of an encapsulated drop as a function of σ. 4 curves at the top-"In-phase" mode. 4 curves at the bottom-"Out-of-phase" mode. Solid lines – oscillation mode number n = 2, dashed lines – n = 3, dash-dotted – n = 4 and dotted – n = 5

8 Conclusions

In this paper, an estimate of the liquids' properties influence on small-amplitude free capillary oscillations of an encapsulated spherical drop has been calculated. Two types of oscillation can be observed, such as "in-phase" type with frequencies higher than those for homogeneous drop (ω_R), and "out-of-phase" type with frequencies significantly lower than ω_R. It is shown that in case of thin outer shell "out-of-phase" type oscillation frequencies decrease up to several times when shell thickness becomes lower. Relation σ between interfacial and free surface tension coefficients has a great influence on the both oscillation types. Lower values of σ result in significant decrease of frequencies ω_n. Relation between densities of inner and outer liquid has almost no effect on "out-of-phase" type, but lowers values of ω_n for "in-phase" type. All the oscillation modes are affected by liquids' properties rather equally, and these dependencies should be taken into account when frequency or drop shape analysis is established. Expressions for encapsulated drop free surface oscillation frequencies with a thin shell of finite thickness were obtained.

Funding Statement: The work of A. Shiryaev was supported by the Russian Science Foundation (Project 19-19-00598 "Hydrodynamics and energetics of drops and droplet jets: formation, motion, break-up, interaction with the contact surface", site: https://www.rscf.ru/).

Conflicts of Interest: The author declares that he has no conflicts of interest to report regarding the present study.

References

1. Patzer, J., Homsy, G. (1975). Hydrodynamic stability of thin spherically concentric fluid shells. *Journal of Colloid and Interface Science, 51(3),* 499–508. DOI 10.1016/0021-9797(75)90146-0.
2. Saffren, M., Elleman, D., Rhim, V. (1982). Normal modes of a compound drop. *Proceedings of the Second International Colloquium on Drops and Bubbles, Monterey, California, November 1981 (D. H. Le Croissette, Ed.), Jet Propulsion Laboratory, California Institute of Technology, Pasadena, CA, 82,* 7.
3. Johnson, R., Sadhal, S. (1985). Fluid mechanics of compound multiphase drops and bubbles. *Annual Review of Fluid Mechanics, 17(1),* 289–320. DOI 10.1146/annurev.fl.17.010185.001445.
4. Lyell, M., Wang, T. (1985). Oscillations of a compound drop system undergoing rotation. *Physics of Fluids, 28(4),* 1023. DOI 10.1063/1.865022.
5. Lyell, M., Wang, T. (1986). Oscillations of a viscous compound drop. *Physics of Fluids, 29(10),* 3481. DOI 10.1063/1.865817.

6. Landman, K. (1985). Stability of a viscous compound fluid drop. *American Institute of Chemical Engineers Journal, 31(4),* 567–573. DOI 10.1002/aic.690310406.
7. Kan, H., Udaykumar, H., Shyy, W., Tran-Son-Tay, R. (1998). Hydrodynamics of a compound drop with application to leukocyte modeling. *Physics of Fluids, 10(4),* 760–774. DOI 10.1063/1.869601.
8. Luo, Z., He, L., Bai, B. (2015). Deformation of spherical compound capsules in simple shear flow. *Journal of Fluid Mechanics, 775,* 77–104. DOI 10.1017/jfm.2015.286.
9. Qu, X., Wang, Y. (2012). Dynamics of concentric and eccentric compound droplets suspended in extensional flows. *Physics of Fluids, 24(12),* 123302. DOI 10.1063/1.4770294.
10. Hua, H., Shin, J., Kim, J. (2014). Dynamics of a compound droplet in shear flow. *International Journal of Heat and Fluid Flow, 50,* 63–71. DOI 10.1016/j.ijheatfluidflow.2014.05.007.
11. Vu, T., Vu, L., Pham, B., Luu, Q. (2018). Numerical investigation of dynamic behavior of a compound drop in shear flow. *Journal of Mechanical Science and Technology, 32(5),* 2111–2117. DOI 10.1007/s12206-018-0420-5.
12. Borthakur, M., Biswas, G., Bandyopadhyay, D. (2018). Dynamics of deformation and pinch-off of a migrating compound droplet in a tube. *Physical Review E, 97(4),* 4. DOI 10.1103/PhysRevE.97.043112.
13. Lind, S., Stansby, P., Rogers, B. (2015). Incompressible-compressible flows with a transient discontinuous interface using smoothed particle hydrodynamics (SPH). *Journal of Computational Physics, 27,* 309–317.
14. Pelekasis, N., Tsamopoulos, J., Manolis, G. (1991). Nonlinear oscillations of liquid shells in zero gravity. *Journal of Fluid Mechanics, 230,* 541–582. DOI 10.1017/S0022112091000897.
15. Kim, S., Kim, J., Cho, J., Weitz, D. (2011). Double-emulsion drops with ultra-thin shells for capsule templates. *Lab on a Chip, 11(18),* 3162–3166. DOI 10.1039/C1LC20434C.
16. Liu, M., Zheng, Y., Li, J., Chen, S., Liu, Y. et al. (2016). Effects of molecular weight of PVA on formation, stability and deformation of compound droplets for ICF polymer shells. *Nuclear Fusion, 57(1),* 016018. DOI 10.1088/0029-5515/57/1/016018.
17. Vian, A., Reuse, B., Amstad, E. (2018). Scalable production of double emulsion drops with thin shells. *Lab on a Chip, 18(13),* 1936–1942. DOI 10.1039/C8LC00282G.
18. Liu, M., Su, L., Li, J., Chen, S., Liu, Y. et al. (2016). Investigation of spherical and concentric mechanism of compound droplets. *Matter and Radiation at Extremes, 1(4),* 213–223. DOI 10.1016/j.mre.2016.07.002.
19. Chekifi, T. (2019). Droplet breakup regime in a cross-junction device with lateral obstacles. *Fluid Dynamics and Materials Processing, 15(5),* 545–555. DOI 10.32604/fdmp.2019.01793.
20. Esmaeeli, A., Behjatian, A. (2017). A note on the transient electrohydrodynamics of a liquid drop. *Fluid Dynamics and Materials Processing, 13(3),* 143–153.
21. Wang, Z., Dong, K., Zhan, S. (2017). Numerical analysis on unsteady internal flow in an evaporating droplet. *Fluid Dynamics and Materials Processing, 13(4),* 221–234.
22. Egry, I. (2005). The oscillation spectrum of a compound drop. *Journal of Materials Science, 40(9),* 2239–2243. DOI 10.1007/s10853-005-1940-9.
23. Egry, I., Ratke, L., Kolbe, M., Chatain, D., Curiotto, S. et al. (2009). Interfacial properties of immiscible Co-Cu alloys. *Journal of Materials Science, 45(8),* 1979–1985. DOI 10.1007/s10853-009-3890-0.
24. Lyubimov, D., Konovalov, V., Lyubimova, T., Egry, I. (2012). Oscillations of a liquid spherical drop encapsulated by a non-concentric spherical layer of dissimilar liquid. *European Journal of Mechanics-B/Fluids, 32,* 80–87. DOI 10.1016/j.euromechflu.2011.11.002.
25. Chashechkin, Y. (2019). Oscillations and short waves on a free falling drop surface (experiment and theory). *Proceedings. Topical Problems of Fluid Mechanics, Prague, February 20–22, 248,* 45–52.
26. Kistovich, A., Chashechkin, Y. (2018). Surface oscillations of a free-falling droplet of an ideal fluid. *Izvestiya Atmospheric and Oceanic Physics, 54(2),* 182–188. DOI 10.1134/S0001433818020123.
27. Testik, F., Barros, A., Bliven, L. (2006). Field observations of multimode raindrop oscillations by high-speed imaging. *Journal of the Atmospheric Sciences, 63(10),* 2663–2668. DOI 10.1175/JAS3773.1.
28. Lord Rayleigh, F. R. S. (1882). On the equilibrium of liquid conducting masses charged with electricity. *Philosophical Magazine, 14(87),* 184–186.

Appendix A. Expressions for the coefficients $\mathbf{C_k(n)}$

$$C_1(n) = (1-n)(2+n) \tag{A.1}$$

$$C_2(n) = \left(\frac{-1}{(1-(1-h)^{2n}+(1-h)^{2n}h)n} + \frac{(1-h)^{-1+n}}{(1-h)^{-2-n}(-1-n)+(1-h)^{n-1}(1+n)}\right) \tag{A.2}$$

$$C_3(n) = \left(\frac{(1-h)^{2+n}}{(1-(1-h)^{2n}+(1-h)^{2n}h)n} - \frac{1}{(1+n)((1-h)^{n-1}-(1-h)^{-2-n})}\right) \tag{A.3}$$

$$C_4(n) = \frac{(1-n)(2+n)\sigma}{(-1+h)^2} \tag{A.4}$$

$$C_5(n) = \left(\frac{(1-h)^{n}}{(1-(1-h)^{2n}+(1-h)^{2n}h)n} - \frac{1}{(1-h)^2(1+n)((1-h)^{-1+n}-(1-h)^{-2-n})}\right) \tag{A.5}$$

$$C_6(n) = \left(-\frac{(1-h)^{2+2n}}{(1-(1-h)^{2n+1})n} + \frac{(1-h)^{-1-n}}{(1+n)((1-h)^{-1+n}-(1-h)^{-2-n})} + \frac{(-1+h)\rho}{n}\right) \tag{A.6}$$